Pergamon

Bioorganic & Medicinal Chemistry 9 (2001) 1753–1764

BIOORGANIC & MEDICINAL CHEMISTRY

Molecular Modeling, Structure–Activity Relationships and Functional Antagonism Studies of 4-Hydroxy-1-methyl-4-(4-methylphenyl)-3-piperidyl 4-Methylphenyl Ketones as a Novel Class of Dopamine Transporter Inhibitors

Shaomeng Wang,[a,*] Sukumar Sakamuri,[b] Istvan J. Enyedy,[a] Alan P. Kozikowski,[b] Wahiduz A. Zaman[c] and Kenneth M. Johnson[c]

[a]*Departments of Oncology and Neuroscience, Georgetown University Medical Center, Building D, Room 235/237 4000 Reservoir Rd, Washington, DC 20007, USA*

[b]*Drug Discovery Program, Department of Neurology, Georgetown University Medical Center, 3900 Reservoir Rd, Washington, DC 20007, USA*

[c]*Department of Pharmacology and Toxicology, University of Texas Medical Branch, Galveston, TX 77555-1031, USA*

Received 6 November 2000; accepted 6 March 2001

Abstract—We previously disclosed the discovery of 4-hydroxy-1-methyl-4-(4-methylphenyl)-3-piperidyl 4-methylphenyl ketone (**3**) as a novel class of dopamine transporter (DAT) inhibitors and showed that (±)-**3** has a significant functional antagonism against cocaine in vitro. Our previous preliminary structure–activity relationship study led to identification of a more potent DAT inhibitor [(±)-**4**] but this compound failed to show any significant functional antagonism. To search for more potent analogues than **3** but still displaying significant functional antagonism, further SARs, molecular modeling studies and in vitro pharmacological evaluation of this novel class of DAT inhibitors were performed. Sixteen new analogues were synthesized in racemic form and evaluated as DAT inhibitors. It was found that seven new analogues are reasonably potent DAT inhibitors with K_i values of 0.041–0.30 and 0.052–0.16 μM in [^{3}H]mazindol binding and inhibition of DA reuptake. Chiral isomers of several potent DAT inhibitors were obtained through chiral HPLC separation and evaluated as inhibitors at all the three monoamine transporter sites. In general, the (−)-isomer is more active than the (+)-isomer in inhibition of DA reuptake and all the (−)-isomers are selective inhibitors at the DAT site. Evaluation of cocaine's effect on dopamine uptake in the presence and absence of (+)-**3** and (−)-**3** showed that (−)-**3** is responsible for the functional antagonism obtained with the original lead (±)-**3**. Out of the new compounds synthesized, analogue (±)-**20**, which is 8- and 3-fold more potent than (±)-**3** in binding and inhibition of DA reuptake, appeared to have improved functional antagonism as compared to (±)-**3**.

Introduction

Cocaine (**1**) is one of the most addictive substances known. Cocaine abuse remains one of the greatest concerns of the American public today, and has therefore become a concern of medical, social, and political leaders. Despite intensive research efforts, development of an effective cocaine therapy remains a difficult task and no specific and effective therapy for the treatment of cocaine abuse is currently available. Recently, the potential pharmacotherapies for treatment of cocaine abuse that are currently being pursued have extensively been reviewed.[1]

Although cocaine (**1**) potently inhibits the reuptake of both norepinephrine (NE) and serotonin (SER) (Table 3), many lines of evidence indicate that its ability to act as a reinforcer stems from its ability to inhibit the reuptake of dopamine (DA) into dopaminergic neurons.[2–9] Cocaine exerts this effect by binding to a specific site on the dopamine transporter (DAT) that can be distinguished from the DA site by mutational analysis.[5] The consequent increase of dopaminergic transmission in the reward mediating brain mesolimbic system is the essence of the dopamine hypothesis of reinforcement advanced by Wise[10] and later elaborated

*Corresponding author. Tel.: +1-202-687-2028; fax: +1-202-687-0617; e-mail: wangs@georgetown.edu

0968-0896/01/$ - see front matter
PII: S0968-0896(01)00090-6

for cocaine by Kuhar.[4] In pursuit of an effective therapy for the treatment of cocaine abuse, significant chemical, biochemical, pharmacological and behavioral studies have been performed on several classes of DAT inhibitors, including cocaine/tropane analogues,[3,11–19] GBR compounds,[20–22] methylphenidate analogues,[23] mazindol analogues,[24] and piperidine-based analogues.[25–29]

We are interested in the discovery of novel DAT inhibitors that can be used as either cocaine antagonists or 'partial agonists'.[30] For this purpose, we have used a novel 3D-database pharmacophore searching approach to discover novel DAT inhibitors.[30] Novel DAT inhibitors are then evaluated as potential cocaine antagonist in an in vitro functional antagonism assay.[30] A DAT inhibitor with a significant functional antagonism suggests that the inhibitor is capable of reducing the binding of cocaine, either by steric hindrance or by an allosteric mechanism, while at the same time having a relatively smaller effect on DA transport. Using this approach, we have recently reported the discovery of hydroxypiperdines as a novel class of DAT inhibitors with significant functional antagonism.[30] Functional antagonism studies showed that the lead compound [(±)-**3**] had the ability to significantly antagonize cocaine's inhibition of DA transport, representing a promising lead for further development. Initial SAR studies led to the identification of a potent analogue [(±)-**4**], with K_i values of 0.011 μM in [^{3}H]mazindol binding and 0.051 μM in inhibition of DA reuptake but with no significant functional antagonism against cocaine.[30] Furthermore, since the antagonism of **3** was originally obtained with its racemic form, it was unclear which stereoisomer is responsible for the observed functional antagonism.

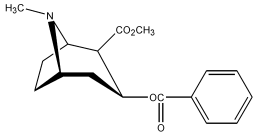

1 (cocaine)

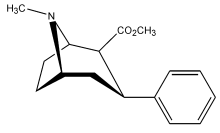

2 (WIN-35065-2)

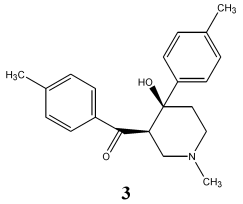

3

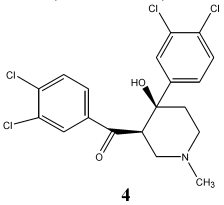

4

The major scopes of this investigation are to better understand the SAR of this novel class of DAT inhibitor and to identify and characterize new analogues with significant functional antagonism.

Results and Discussion

SARs of racemic compounds in inhibition of DA reuptake

A total of 16 new analogues were synthesized in racemic form and tested as inhibitors at the DAT site for their uptake activities. The structures of these analogues (**12**–**27**) are shown in Table 1 and their activities are summarized in Table 2. For purpose of comparison, the structures and activities of nine analogues (**3**–**11**) from our previous study,[30] including the lead compound **3**, are also included in the tables.

Table 1. Chemical structures of piperidinols

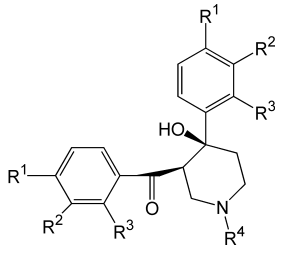

Compound	R^1	R^2	R^3	R^4
3	Me	H	H	Me
4	Cl	Cl	H	Me
5	H	H	H	Me
6	F	H	H	Me
7	Cl	H	Cl	Me
8	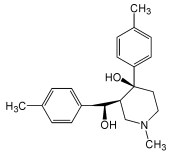			
9	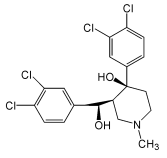			
10	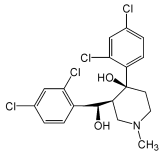			
11	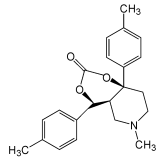			
12	Cl	H	H	Me
13	Br	H	H	Me
14	I	H	H	Me
15	Ethyl	H	H	Me
16	H	H	Cl	Me
17	H	Cl	H	Me
18	F	F	H	Me
19	Me	Me	H	Me
20	Cl	Me	H	Me
21	Me	H	H	Ethyl
22	Cl	H	H	Ethyl
23	Cl	Cl	H	Ethyl
24	Cl	Cl	H	$(CH_2)_2Ph$
25	Br	H	H	$(CH_2)_2Ph$
26	Cl	Cl	H	$(CH_2)_3Ph$
27	Br	H	H	$(CH_2)_3Ph$

Table 2. The activity of racemic compounds in inhibition of DA reuptake

Compound	K_i (μM) [^{3}H]-DA uptake
1[a]	0.27±0.02[b]
3[a]	0.36±0.03
4[a]	0.051±0.008
5[a]	2.59±0.23
6[a]	4.20±0.07
7[a]	5.85±1.08
8[a]	15.80±0.65
9[a]	4.22±0.02
10[a]	7.52±0.09
11[a]	9.48±0.74
12	0.16±0.02
13	0.085±0.019
14	0.12±0.00
15	8.09±0.53
16	23.34±1.06
17	0.16±0.01
18	0.89±0.10
19	0.10±0.01
20	0.11±0.02
21	1.14±0.03
22	0.57±0.03
23	0.052±0.004
24	0.39±0.01
25	1.49±0.01
26	0.50±0.02
27	1.40±0.15

[a]Data taken from ref 30.
[b]Mean ± standard error of 2–3 experiments, each conducted using six concentrations of drug in triplicate.

The compounds were synthesized using known methods from the literature. All substituted acetophenones were purchased from commercial suppliers, except compound **29**, which was prepared in 90% yield by reacting the substituted phenacyl chloride **28** with $SnCl_2$ and NaI in a 5:1 mixture of THF and H_2O for 2 h (Scheme 1).[35] The general synthesis of the compounds **12**–**27** is illustrated in Scheme 2. Briefly, reaction of an amine hydrochloride with an excess of an aryl methyl ketone (**29**–**44**) and paraformaldehyde in the presence of a catalytic amount of hydrochloric acid led to compounds **12**–**27** (Scheme 2).[36]

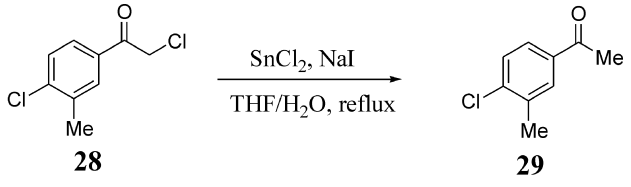

28 **29**

Scheme 1. Synthesis of intermediate **29**.

Our preliminary SAR studies suggested that the substituents on each phenyl ring have considerable influence on their binding and uptake activities.[30] To gain a better understanding of the effects of phenyl substitutions, analogues **12**–**20** were made and tested. Lead compound **3** with a *p*-methyl substituent in both phenyl rings has a K_i value of 0.36 μM in inhibition of DA uptake. A *p*-fluoro substituent in both phenyl rings resulted in an analogue (**6**) with a K_i value of 4.20 μM in inhibition of DA reuptake, approximately 12-fold less potent than **3**, suggesting that a substituent at the *para* position of both phenyl rings has a significant effect on the uptake activity. To investigate further this effect, analogues **12**–**15** were synthesized and evaluated. A *p*-chloro substituent in both phenyl rings resulted in analogue **12** with a K_i value of 0.16 μM in inhibition of DA reuptake, approximately 2 times more potent than **3**. Compared to the unsubstituted analogue **5**, the *p*-chloro substituent in both phenyl rings improved the activity in inhibition of DA reuptake by 16-fold. Analogue **13** with a *p*-bromo substituent in both phenyl rings has a K_i value of 0.085 μM in inhibition of DA uptake, representing a 30-fold improvement compared to the unsubstituted analogue **5**. A *p*-iodo substituent in both phenyl rings resulted in analogue **14**, with a K_i value of 0.124 μM in inhibition of DA uptake, a 21-fold improvement compared to the unsubstituted analogue **5** but slightly less potent than **13** with a *p*-bromo substituent in both phenyl rings. Analogue **15** with a *p*-ethyl substituent in both phenyl rings has a K_i value of 8.09 μM in inhibition of DA uptake, a 22-fold loss in activity as compared to the lead compound **3** with a *p*-methyl substituent. Therefore, a bromo atom appears to be optimal to achieving the highest potency in inhibition of DA reuptake among analogues **3**, **5**, **6**, **12**, **13**, **14**, and **15** with a mono substituent at the *para* position in both phenyl rings.

To investigate the effect of the substitution positions (*ortho*, *meta*, and *para*) in the phenyl rings, two analogues, **16** and **17** with a mono chloro substituent at either the *ortho* or *meta* position in both phenyl rings were synthesized. They were tested as inhibitors of DA reuptake and compared to analogue **12** with a chloro substituent at the *para* position in both phenyl rings. Analogue **16** with a chloro substituent at the *ortho* position in both phenyl rings has a K_i value of 23.34 μM in inhibition of DA uptake, a 65-fold less potent than analogue **12**. Analogue **17** with a chloro substituent at the *meta* position in both phenyl rings has a K_i value of 0.16 μM in inhibition of DA uptake, comparable to the

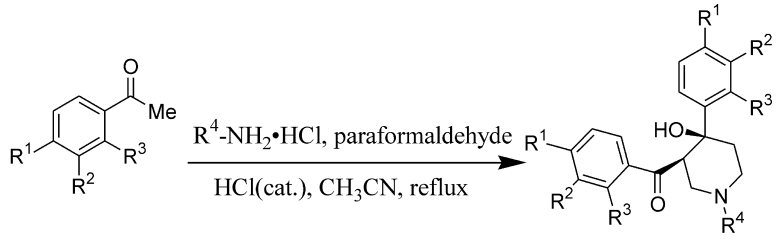

29-44 **12-27**

Scheme 2. Synthesis of analogues **12**–**27**.

activity of analogue **12**. Since **12**, **16**, and **17** have very similar hydrophobicity, the difference between **12**, **16**, and **17** in their activities in inhibition of DA reuptake is likely due to their difference in conformational profiles and this has been further investigated through our molecular modeling studies (see Molecular Modeling).

Our previous SAR studies led to the identification of a potent analogue (**4**) with 3,4-dichloro substituents in both phenyl rings.[30] To explore further the SARs of compounds with two substituents in both phenyl rings, analogues **18**, **19**, and **20** were made and tested. Analogue **18** with 3,4-difluoro substituents has a K_i value of 0.89 μM in the inhibition of DA uptake, a 5-fold improvement as compared to the 4-fluoro, mono-substituted analogue **6** but 17-times less potent than the **3**, 4-dichloro substituted analogue **4**. Analogue **19** with 3,4-dimethyl substituents has a K_i value of 0.10 μM in inhibition of DA uptake, only 2-fold less potent than **4**. It is interesting to note that as compared to the 3,4-dichloro substituted analogue **4**, the activity of **19** in inhibition of the reuptake of DA is only 2-fold less potent, but the binding affinity for the [^{3}H]mazindol site is reduced by 28-fold (Table 3). Analogue **20** with 4-chloro-3-methyl-substituents has a K_i value of 0.11 μM in inhibition of DA uptake, 2-fold less potent than **4** but 3-fold more potent than the lead compound **3**.

Previous investigations of a tropane series of compounds showed that fairly large *N*-substituents may be tolerated for their activity in inhibition of DA reuptake.[31,32] To investigate the effect of *N*-substitutions in this class of DAT inhibitors, a series of analogues were synthesized and tested (**21**–**27**). In contrast to the SAR of tropane analogues,[31,32] replacement of the *N*-methyl group with larger substituents in general decreases the activity in inhibition of the reuptake of DA in this class of compounds. Analogue **21** with a *N*-ethyl substituent and a 4-methyl substituent at both phenyl rings has a K_i value of 1.14 μM in inhibition of DA uptake, 3-fold less potent than its corresponding *N*-methyl analogue **3**. Analogue **22** with a *N*-ethyl substituent and a 4-Cl substituent at both phenyl rings has a K_i value of 0.57 μM in inhibition of DA uptake, 4-fold less potent than its corresponding *N*-methyl analogue **12**. The only exception is analogue **23** with a *N*-ethyl substituent and 3,4-dichloro substituents in both phenyl rings, which has a K_i value of 0.052 μM in inhibition of DA uptake, as potent as its corresponding *N*-methyl analogue **4** (K_i equal to 0.051 μM). With larger *N*-substituents, the potency of the analogues decreases even more. Analogue **24** with a *N*-ethylphenyl substituent and 3,4-dichloro substituents in both phenyl rings has a K_i value of 0.39 μM, 8-fold less potent than its corresponding *N*-methyl analogue **4**. Analogue **25** with a *N*-ethylphenyl substituent and a 4-bromo substituent in both phenyl rings has a K_i value of 1.49 μM, 18-fold less potent than its corresponding *N*-methyl analogue **13**. Analogue **26** with a *N*-propylphenyl substituent and 3,4-dichloro substituents in both phenyl rings has a K_i value of 0.50 μM, 10-fold less potent than its corresponding *N*-methyl analogue **4**. Analogue **27** with *N*-propylphenyl substituent and a 4-bromo substituent in both phenyl rings has a K_i value of 1.40 μM, 17-fold less potent than its corresponding *N*-methyl analogue **13**. Therefore, it appeared that a *N*-methyl substituent is optimal for the activity in inhibition of DA reuptake with this class of compounds.

Selectivity of potent racemic compounds at the three monoamine transporters (DAT, SERT, and NET)

Cocaine potently inhibits the reuptake of DA, but even more potently inhibits the reuptake of serotonin (SER) and norepinephrine (NE) (Table 3). To assess the selectivity of several potent analogues (**12**, **13**, **17**, **19**, **20**, and **23**), we evaluated them as reuptake inhibitors at SERT and NET sites and the results are summarized in Table 3. The selectivity between DAT relative to SERT for analogues **4**, **12**, **13**, **17**, **19**, **20**, and **23** is 47-, 6-, 22-, 3-, 8-, 10-, and 43-fold, respectively. Thus, analogues **4** and **23** have the best selectivity between DAT and SERT, being 47- and 43-fold, respectively. The selectivity between DAT and NET for analogues **4**, **12**, **13**, **17**, **19**, **20**, and **23** is 4-, 8-, 22-, 3-, 8-, 6-, and 11-fold, respectively. Therefore, in contrast to cocaine, in general, these inhibitors are more potent at the DAT site among these three transporter sites.

Table 3. The activities and selectivity of selected racemic compounds at three monoamine transporter sites

Compound	K_i (μM)				Selectivity	
	Binding	Uptake			SER	NE
	([^{3}H]-Mazindol)	([^{3}H]-DA)	([^{3}H]-SER)	([^{3}H]-NE)	DA	DA
1[a] (cocaine)	0.23±0.02[b]	0.27±0.02	0.16±0.00	0.11±0.01	0.6	0.4
3[a]	0.49±0.03	0.36±0.03	1.63±0.15	3.86±0.07	4.5	10.7
4[a]	0.011±0.001	0.051±0.008	2.38±0.01	0.18±0.05	46.7	3.5
12	0.25±0.01	0.16±0.02	0.93±0.01	1.21±0.06	5.8	7.6
13	0.23±0.05	0.085±0.019	1.88±0.19	1.86±0.09	22.1	21.9
17	0.16±0.01	0.16±0.01	0.46±0.04	0.43±0.08	2.9	2.8
19	0.30±0.03	0.10±0.01	0.81±0.01	1.01±0.09	8.0	10.0
20	0.059±0.013	0.11±0.02	1.16±0.11	0.64±0.06	10.4	5.7
23	0.041±0.001	0.052±0.004	2.22±0.19	0.61±0.11	42.7	11.7

[a]Data taken from ref 30.
[b]Mean ± standard error of 2–3 experiments, each conducted using six concentrations of drug in triplicate.

SARs of enantiomers and their selectivity at the three transporter sites

Each of these compounds shown in Table 1 was synthesized in racemic form and the results are somewhat complicated by the presence of two stereoisomers. To solve this problem, we obtained the individual enantiomers of 4 potent analogues, **3** (the lead compound), **4** (the most potent analogue), **19** and **20** (potent analogues possessing significant cocaine antagonism) through chiral HPLC separation (see Experimental). These enantiomers were then evaluated as inhibitors at all the three transporter sites and the results are summarized in Table 4.

Overall, the (−)-isomers are more potent inhibitors than the (+)-isomers at the DAT site with each compound. Thus, the (−)-isomer for each compound has an activity in inhibition of DA reuptake approximately 2-fold greater than its respective racemic form. The difference in activities between the (+)- and (−)-isomers in inhibition of DA reuptake is fairly large for **3** and **19**, being 7.6- and 10.8-fold, respectively. Interestingly, the difference between the (+)- and (−)-isomers is relatively small for **4** and **20**, being only 1.4- and 2.5-fold, respectively. Comparison between their structures showed that **3** and **19** have a *para*-methyl substituent in each phenyl ring, while **4** and **20** have a *para*-Cl substituent in each phenyl ring. Replacement of the *para*-methyl group in **19** with the *para*-Cl group resulted in **20**. The improvement in activities in inhibition of DA reuptake is 7.0-fold from (+)-**19** to (+)-**20** but is only 1.6-fold from (−)-**19** to (−)-**20**. These results suggested that (+)- and (−)-isomers may bind to the DAT in different manner and a *para*-Cl group in each phenyl ring more significantly improves the potency for the (+)-isomers than for the (−)-isomers.

Furthermore, the (+)- and (−)-isomers have different selectivity profiles among the three transporters, especially for **3** and **19**. While (+)-**3** is only marginally selective for DAT, (−)-**3** is quite selective for DAT, with a selectivity of 7.3-fold between DAT and SERT sites and 33.7-fold between DAT and NET sites. Analogue (+)-**19** isomer is in fact more selective for SERT, but (−)-**19** is fairly selective for DAT. Both the (+)- and (−)-isomers of **4** and **20** are selective for DAT, suggesting the *para*-Cl substitutent in each phenyl ring in these two compounds is a favorable binding element for the DAT and/or an unfavorable binding element relative to the SERT and NET sites.

Molecular Modeling Studies

Our SAR studies showed that the nature and the position of the substituent(s) on both phenyl rings play an important role in the binding and reuptake activities for this class of compounds. To achieve a better understanding of factors important to their activities and to guide our further design of new analogues, we have carried molecular modeling studies. Based upon the data obtained for eight chiral compounds (Table 4), the (−)-isomer is always the more active compound between the two isomers and its activity is approximately 2 times more potent than its racemic form. Because we have much more extensive SAR with the racemic compounds and have very limited data on chiral compounds, molecular modeling study was based upon the activity in inhibition of DA reuptake of the racemic compounds. However, the molecular modeling results based upon the SARs of the racemic compounds should be applicable to both racemic compounds and their (−)-isomers.

Analogues **12**, **16**, and **17** all have a mono chloro substituent on each phenyl ring. While **12** and **17** have similar activities in inhibition of the reuptake of DA (K_i values of 0.160 and 0.155 μM respectively), **16** (K_i value of 23.34 μM) is approximately 150-fold less potent than **12** and **17**. Since **12**, **16** and **17** only differ in the position of the chloro substituent in both phenyl rings and have similar size and hydrophobicity, the substantial difference in their activities is thus likely due to their conformational preferences. Conformational analysis showed that the lead compound **3**, analogues **12** and **17** have virtually identical conformational profiles (i.e., they have essentially identical lowest energy conformations and also have similar low minimum conformations). The superposition of **3** and **12** in their lowest energy conformations is shown in Figure 1A. However, analogue **16** has a significantly different conformational profile from **3**, **12**, and **17**. In its lowest energy conformation of **16**, the phenyl ring attached to the carbonyl group adopts a significantly different orientation from that in **3**, **12**, and **17**, deviated by approximately 40°. The

Table 4. Activities of chiral isomers of several potent inhibitors at the three transporter sites

Compound	K_i (nM)				Selectivity	
	Binding	Uptake			SER	NE
	([^{3}H]-Mazindol)	([^{3}H]-DA)	([^{3}H]-SER)	([^{3}H]-NE)	DA	DA
(+)-**3**	1.93±0.20	1.64±0.22	0.62±0.03	5.17±0.44	2.5	2.9
(−)-**3**	0.27±0.01	0.22±0.02	1.58±0.02	7.27±1.32	7.3	33.7
(+)-**4**	0.020±0.002	0.051±0.007	1.12±0.10	0.38±0.04	21.9	7.4
(−)-**4**	0.013±0.002	0.037±0.002	0.90±0.09	0.18±0.01	24.2	4.9
(+)-**19**	1.57±2.00	0.78±0.13	0.37±0.01	3.55±0.07	0.5	4.6
(−)-**19**	0.060±0.003	0.072±0.005	0.497±0.05	0.79±0.08	6.9	10.8
(+)-**20**	0.082±0.014	0.11±0.01	0.97±0.09	0.55±0.04	8.8	4.9
(−)-**20**	0.022±0.005	0.045±0.008	0.93±0.05	0.52±0.07	21	11

superposition of **3** and **16** in their lowest energy conformations is shown in Figure 1B. In order to adopt the same orientation as that in **3**, **12** and **17**, analogue **16** would have to pay an energy penalty as much as 9 kcal/mol. Therefore, although it is not absolutely certain that the lowest energy conformations of **3**, **12**, and **17** must be their active conformation in binding to the DAT, our results suggest that conformational preference of these compounds plays an important role for their activity in inhibition of the reuptake of DA.

Our SAR studies showed that among the analogues with a mono substituent at the *para* position in both phenyl rings, the nature of the substitutent has a significant effect on the activity. For example, while **13** with a *p*-bromo substituent has a K_i value of 0.085 μM in inhibition of DA reuptake, **15** with a *p*-ethyl substituent has a K_i value of 8.09 μM, 95-fold less potent than **13**. Conformational analysis of these compounds showed that they have virtually identical conformational profiles, suggesting that their difference in activity is not due to their conformational difference. Examination of these substituents showed that they differ in size, hydrophobicity and electronic properties. To investigate if their size and hydrophobicity play a role in determining their activity in inhibition of the reuptake of DA, we calculated the size (volume, V_m) and hydrophobicity (partition coefficient between *n*-octanol and water, logP) value for these seven mono-substituted analogues and the data are provided in Table 5.

Using the genetic function approximation algorithm[42] implemented in the Cerius2 program,[41] several quantitative models were obtained for these seven analogues with a mono substituent at the *para* position in both phenyl rings. A strong parabolic correlation [eq (1)] was found between the K_i value for reuptake of DA and the size of these seven compounds. The optimal value for V_m is 322.4 Å^3, approximately equal to the volume of compound **13** with a bromo substituent.

$$\log(\frac{1}{K_i}) = 6.79 - 0.0013 \times (V_m - 322.4)^2 \quad (1)$$

$$N = 7,\ r^2 = 0.76,\ F = 15.5,\ LOF = 0.42$$

The correlation between AlogP (the calculated logP value) and the K_i for reuptake of DA is, however, only marginal [$r^2 = 0.25$; eq (2)].

$$\log(\frac{1}{K_i}) = 2.49 + 1.66\text{AlogP} - 0.17(\text{AlogP})^2 \quad (2)$$

$$N = 7,\ r^2 = 0.25,\ F = 0.65,\ LOF = 2.32$$

When using these two parameters, the best equation [eq (3)] obtained has a marginal improvement as compared to eq (1) using the volume alone.

$$\log(\frac{1}{K_i}) = 4.67 - 0.0011 \times (V_m - 312.7)^2 + 0.57\text{AlogP}$$
$$N = 7,\ r^2 = 0.89,\ F = 15.6,\ LOF = 0.79 \quad (3)$$

Furthermore, we have investigated if electronic terms such as the sum of atomic polarizabilities and the dipole moment may play a role. We found that inclusion of these two terms in the QSAR analysis does not improve the quality of the QSAR model (data not shown). Thus, based upon our analyses, the size of the substituents plays an important role in determining their potency in inhibition of the reuptake of DA for analogues with a mono substituent at the *para* position in both phenyl rings, while the hydrophobicity (logP) play a less significant role. Taken together, the results obtained from current and previous studies[30] indicated that for this class of compounds, the pharmacophore, the conformational preference and the substituent size in the phenyl rings play important roles in determining their affinity for the DA reuptake site.

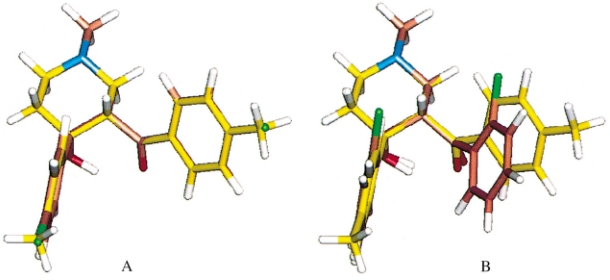

Figure 1. Superposition of the lowest energy conformations: (A) lead compound **3** (yellow), on analogue **12** (brown); (B) lead compound **3** (yellow) on analogue **16** (brown).

Table 5. Calculated hydrophobicity (AlogP) and volume of *para*, mono-substituted analogues used in the QSAR analysis

Analogue	Substituent	–log K_i	V_m	ALogP
5	H	5.59	286.0	2.42
3	CH_3	6.44	319.1	3.35
6	F	5.38	295.3	2.70
12	Cl	6.80	312.7	3.46
13	Br	7.07	322.4	4.00
14	I	6.91	334.0	4.93
15	CH_3CH_2	5.09	353.5	4.15

Functional Antagonism

In our previous study, the lead compound **3** was shown to display a significant functional antagonism but **4**, a more potent analogue, failed to show significant functional antagonism. To search for more potent analogues than **3** that possess significant functional antagonism, a number of more potent new analogues synthesized in the present study were evaluated for their cocaine

antagonism using an in vitro functional assay.[30] For the purpose of comparison, the functional antagonism of cocaine against cocaine was also determined using unlabeled cocaine (cold cocaine). The results are summarized in Table 6. Among the four new analogues evaluated, analogues **12** and **20** showed significant functional antagonism and **20** appeared to have an improved functional antagonism as compared to **3**. For example, the experimental IC_{50} of cocaine in inhibition of DA reuptake in the presence of 30 nM of **20** is 775 nM and this value is 213% of the calculated theoretical value of 363 nM using the same binding site model. The experimental IC_{50} of cocaine in inhibition of DA reuptake in the presence of 100 nM of **20** was 945 nM and this value is 176% of the calculated theoretical value of 538 nM using the same binding site model. Very interestingly, cocaine itself has a very moderate functional antagonism in this assay. Using 50 nM of cold cocaine, the experimental IC_{50} value of the labeled cocaine is 415 nM, which is 122% of the theoretical IC_{50} value calculated using the same site binding model. Similarly, using 100 nM of cold cocaine, the experimental IC_{50} value of the labeled cocaine is 511 nM, which is 131% of the calculated theoretical IC_{50} value using the same site binding model. The moderate antagonism of cold cocaine may be attributed to the fact that cocaine binds to two different binding sites at the DAT. Thus, as compared to **3** and cocaine itself, analogues **20**, a more potent DAT inhibitor than **3** and cocaine, displays a significant in vitro functional antagonism.

The functional antagonism of **3** and **20** was obtained with their racemates and it was not clear which chiral isomer is responsible for the observed functional antagonism. Thus, we have evaluated the functional antagonism of the two stereoisomers of **3** and **20** in the functional assay and the results are summarized in Table 7. At concentrations of 50 and 200 nM of (±)-**3**, (+)-**3** and (−)-**3** isomers presumably have 25 and 100 nM each in the mixture. Based upon their activity in inhibition of DA reuptake (Table 4), at these concentrations, only (−)-**3** has a significant activity in binding to DAT, while (+)-**3** has a minimal activity. Hence, it is predicted that the functional antagonism of (±)-**3** may be primarily due to the (−)-**3** isomer. Since (−)-**3** is approximately 2 times more potent than (±)-**3** in inhibition of DA uptake, we tested the functional antagonism of (−)-**3** at 30 and 100 nM in order to compare directly with the functional antagonism of (±)-**3** obtained at 50 and 200 nM. As can be seen from Table 7, (−)-**3** and (±)-**3** have similar functional antagonism at concentrations that produce similar inhibition of DA reuptake, indicating that the functional antagonism observed for (±)-**3** at concentrations of 50 and 200 nM is primarily due to the functional antagonism of the (−)-**3** isomer. However, (+)-**3** also has significant functional antagonism, although this isomer is a much weaker DAT inhibitor. Although the chiral isomer (−)-**20** is twice as potent as (+)-**20** in inhibition of DA reuptake, both isomers are reasonably potent DAT inhibitors with K_i values of 45 and 111 nM, respectively. These two isomers were evaluated for the functional antagonism. As can be seen from Table 7, both (−)-**20** and (+)-**20** have similar functional antagonism. It should be noted that no direct relationship between the potency in inhibition of DA reuptake of a compound and its functional antagonism was observed and the precise underlying molecular mechanism for the observed functional antagonism is not entirely clear.

Summary

To further explore the SARs of 4-hydroxy-1-methyl-4-(4-methylphenyl)-3-piperidyl 4-methylphenyl ketones as a novel class of DAT inhibitors and to search for more potent analogues than the lead compound that possess significant functional antagonism, 16 new analogues were synthesized in racemic form and evaluated as DAT inhibitors. It was found that seven new analogues are reasonably potent DAT inhibitors with K_i values of 0.052 to 0.16 μM in inhibition of DA reuptake. Molecular modeling studies showed that the pharmacophore, the conformational preference and the substituent size in the phenyl rings play important roles in determining their affinity for the DA reuptake site.

Chiral isomers of several potent DAT inhibitors were obtained through chiral HPLC separation and evaluated as inhibitors at the three monoamine transporter sites. In general, the (−)-isomer is more active than the (+)-isomer in inhibition of DA reuptake and all the (−)-isomers of potent analogues are selective inhibitors at the DAT site. Evaluation of cocaine's effect on dopamine uptake in the presence and absence of (+)-**3** and (−)-**3** showed that (−)-**3** is responsible for the functional antagonism obtained with the original lead (±)-**3**, although both isomers display significant functional antagonism. Out of the new compounds synthesized, analogue (±)-**20**, which is 8- and 3-fold more potent than (±)-**3** in binding and inhibition of DA reuptake, appeared to have improved functional antagonism as compared to (±)-**3**. Both stereoisomers of (±)-**20** display significant functional antagonism. Therefore, analogue **20** represent a potential cocaine antagonist for further evaluations. Further pharmacological and behavioral studies are currently under way to investigate the mechanism of its functional antagonism and its therapeutic potential for the treatment of cocaine abuse.

Experimental

Molecular modeling

Conformational analysis was performed using the conformational analysis module in the QUANTA program.[38] Generally, if a compound has fewer than five rotatable single bonds, the grid scan conformational search protocol was employed. In this protocol, each rotatable bond was systematically rotated to generate a starting conformation, which was subsequently minimized using the CHARMm program[39] within QUANTA. If a compound has more than five rotatable

Table 6. Functional antagonism of racemate compounds against cocaine

Drugs	IC_{50} (nM) [^{3}H]-Dopamine uptake (Experimental)	IC_{50} (nM) [^{3}H]-Dopamine uptake (Theoretical)
Cocaine alone	297 ± 22[a]	
Cocaine + cold cocaine (50 nM)	415 ± 30	339 ± 11
Cocaine + cold cocaine (100 nM)	511 ± 28	390 ± 14
Cocaine + (±)-**3** (50 nM)	470 ± 25	331 ± 11
Cocaine + (±)-**3** (200 nM)	717 ± 49	438 ± 22
Cocaine + (±)-**4** (10 nM)	382 ± 13	346 ± 17
Cocaine + (±)-**4** (50 nM)	647 ± 75	567 ± 32
Cocaine + (±)-**12** (50 nM)	506 ± 8	379 ± 19
Cocaine + (±)-**12** (100 nM)	616 ± 38	466 ± 24
Cocaine + (±)-**19** (30 nM)	463 ± 11	373 ± 20
Cocaine + (±)-**19** (75 nM)	595 ± 45	483 ± 23
Cocaine + (±)-**20** (30 nM)	775 ± 17	363 ± 18
Cocaine + (±)-**20** (100 nM)	945 ± 97	538 ± 29
Cocaine + (±)-**23** (10 nM)	453 ± 20	344 ± 18
Cocaine + (±)-**23** (30 nM)	555 ± 38	451 ± 23

[a]SE was based upon 2–3 experiments.

Table 7. Functional antagonism of chiral isomers against cocaine

Drugs	IC_{50} (nM) [^{3}H]-Dopamine uptake (Experimental)	IC_{50} (nM) [^{3}H]-Dopamine uptake (Theoretical)
Cocaine alone	297 ± 22[a]	
Cocaine + cold cocaine (50 nM)	415 ± 30	339 ± 11
Cocaine + cold cocaine (100 nM)	511 ± 28	390 ± 14
Cocaine + (−)-**3** (30 nM)	482 ± 8	329 ± 16
Cocaine + (−)-**3** (100 nM)	663 ± 20	430 ± 22
Cocaine + (+)-**3** (300 nM)	464 ± 2	343 ± 17
Cocaine + (+)-**3** (1000 nM)	701 ± 58	461 ± 24
Cocaine + (−)-**20** (10 nM)	483 ± 12	345 ± 18
Cocaine + (−)-**20** (30 nM)	647 ± 11	479 ± 27
Cocaine + (+)-**20** (10 nM)	451 ± 20	328 ± 13
Cocaine + (+)-**20** (30 nM)	564 ± 32	365 ± 18

[a]SE was based upon 2–3 experiments.

bonds, a random sampling protocol was used to generate conformations. Up to 5000 conformations were generated and minimized. Energy minimization of each conformation was computed with 5000 iterations or until convergence, defined as an energy gradient of 0.001 kcal mol^{-1} Å^{-1} or less. An adopted basis Newton–Raphson algorithm, implemented in the CHARMm program, was used for energy minimization. A constant dielectric constant (equal to 1) was used throughout all the calculations. Upon the completion of conformation generation and energy minimization, the most stable conformation was identified (the global minimum in vacuum). It is noted, however, that the lowest energy conformation may not be the bioactive conformation, as was shown previously.[40] For this reason, other low energy conformations, typically within 5 kcal/mol of the global minimum were identified. Cluster analysis was performed to determine the number of truly unique conformations (clusters), using the cluster analysis module available in the QUANTA program. These low energy conformational clusters together are likely to include the bioactive conformations for a compound.

QSARs were derived using the genetic approximation algorithm[42] as implemented in the QSAR module of the Cerius^2 molecular modeling package.[41] The partition coefficient between *n*-octanol and water (logP) values were calculated using the ALOGP method,[43] as implemented in the Cerius^2 molecular modeling package. The molecular volume was calculated using the QSAR module as implemented in the Cerius^2 molecular modeling package.

Chemistry

General methods. THF was freshly distilled under nitrogen from sodium benzophenone. ^{1}H and ^{13}C NMR spectra were obtained with a Varian Unity Inova instrument at 300 and 75.46 MHz, respectively. ^{1}H chemical shifts (δ) are reported in ppm downfield from internal TMS. ^{13}C chemical shifts are referenced to $CDCl_3$ (central peak, δ = 77.0 ppm). Melting points were determined in Pyrex capillaries with a Thomas–Hoover Unimelt apparatus and are uncorrected. Mass spectra were measured in the EI mode at an ionization potential of 70 eV. TLC was performed on Merck silica gel $60F_{254}$ glass plates; column chromatography was performed using Merck silica gel (60–200 mesh). The following abbreviations are used: THF = tetrahydrofuran; DCM = dichloromethane; ether = diethyl ether.

4-Chloro-3-methylacetophenone (29). A solution of 4-chloro-3-methyl phenacylchloride (**28**) (4.8 g, 23.6 mmol), sodium iodide (14.2 g, 94.6 mmol) and $SnCl_2$ (14.4 g, 75.7 mmol) in a 5:1 mixture of THF and H_2O was refluxed for 2 h and cooled to room tempera-

ture. The organic layer was separated, and the aqueous layer was extracted with ether. The combined organic layers were dried (Na_2SO_4), concentrated, and purified by passing through a small bed of silica gel using ether as eluent to afford the title compound as a colorless liquid (3.55 g, 90%). ^{1}H NMR ($CDCl_3$) δ 2.42 (3H, s), 2.60 (3H, s), 7.42 (1H, d, J = 8.3 Hz), 7.72 (1H, dd, J = 8.3, 1.7 Hz), 7.83 (1H, s); ^{13}C NMR ($CDCl_3$) δ 20.0, 26.5, 127.0, 129.1, 130.6, 135.4, 136.4, 139.6, 197.1. Anal. (C_9H_9ClO) C, H, N.

General procedure for the synthesis of compounds 12–27. To an equimolar mixture of aryl methyl ketone and paraformaldehyde in acetonitrile (15 mL/g of ketone), was added amine hydrochloride (0.25 equiv), and the mixture was refluxed for 20 h in the presence of a catalytic amount of hydrochloric acid (37% w/v, 0.02 mL/1 g of ketone). The reaction mixture was cooled to room temperature, and volatiles were removed under reduced pressure. The resulting mass was dissolved in DCM, washed with aq $NaHCO_3$ solution, water, and brine, dried (Na_2SO_4), and concentrated under reduced pressure. The crude compounds were purified by column chromatography using triethylamine/diethyl ether as eluent to afford the following compounds:

4-Chlorophenyl 4-(4-chlorophenyl)-4-hydroxy-1-methyl-3-piperidyl ketone (12). White solid; yield 88%; mp 168–170 °C. ^{1}H NMR ($CDCl_3$) δ 1.82 (1H, br t, J = 13.9 Hz), 1.94–2.07 (1H, m), 2.41 (3H, s), 2.64–2.73 (2H, m), 2.80 (1H, br d, J = 7.1 Hz), 2.90 (1H, dd, J = 11.2, 2.7 Hz), 4.30 (1H, dd, J = 11.5, 3.7 Hz), 5.10 (1H, d, J = 2.7 Hz), 7.22 (2H, d, J = 8.6 Hz), 7.42 (4H, dd, J = 8.8, 2.9 Hz), 7.82 (2H, d, J = 8.5 Hz); ^{13}C NMR ($CDCl_3$) δ 39.8, 45.2, 50.5, 51.2, 54.5, 72.3, 125.9, 128.4, 129.2, 129.6, 132.6, 133.9, 140.8, 145.5, 202.7. Anal. ($C_{19}H_{19}Cl_2NO_2$) C, H, N.

4-Bromophenyl 4-(4-bromophenyl)-4-hydroxy-1-methyl-3-piperidyl hetone (13). Yellow solid; yield 74%; mp 181 °C. ^{1}H NMR ($CDCl_3$) δ 1.80 (1H, br d, J = 13.9 Hz), 1.96–2.08 (1H, m), 2.40 (3H, s), 2.66 (2H, t, J = 11.2 Hz), 2.78 (1H, br d, J = 7.5 Hz), 2.90 (1H, dd, J = 11.3, 3.2 Hz), 4.28 (1H, dd, J = 11.3, 3.4 Hz), 5.08 (1H, d, J = 2.2 Hz), 7.29–7.40 (4H, m), 7.58 (2H, d, J = 8.3 Hz), 7.75 (2H, d, J = 8.3 Hz); ^{13}C NMR ($CDCl_3$) δ 39.8, 45.9, 50.4, 51.1, 54.4, 72.3, 120.8, 126.3, 129.6, 129.7, 131.4, 132.2, 134.3, 146.0, 202.9. Anal. ($C_{19}H_{19}Br_2NO_2$) C, H, N.

4-Hydroxy-4-(4-iodophenyl)-1-methyl-3-piperidyl 4-iodophenyl ketone (14). Light-yellow solid; yield 66%; mp 176 °C. ^{1}H NMR ($CDCl_3$) δ 1.80 (1H, br d, J = 14.0 Hz), 1.95–2.03 (1H, m), 2.40 (3H, s), 2.62–2.71 (2H, m), 2.78 (1H, br d, J = 7.5 Hz), 2.90 (1H, dd, J = 11.0, 3.2 Hz), 4.26 (1H, dd, J = 11.5, 3.4 Hz), 5.06 (1H, d, J = 2.4 Hz), 7.22 (2H, d, J = 8.3 Hz), 7.58 (4H, d, J = 8.3 Hz), 7.82 (2H, d, J = 8.3 Hz); ^{13}C NMR ($CDCl_3$) δ 39.8, 45.9, 50.3, 51.1, 54.4, 72.4, 92.5, 102.6, 126.6, 129.5, 134.8, 137.3, 138.2, 146.8, 203.2. Anal. ($C_{19}H_{19}I_2NO_2$) C, H, N.

4-Ethylphenyl 4-(4-ethylphenyl)-4-hydroxy-1-methyl-3-piperidyl ketone (15). Colorless thick syrup; yield 78%. ^{1}H NMR ($CDCl_3$) δ 1.16 (3H, t, J = 7.6 Hz), 1.25 (3H, t, J = 7.5 Hz), 1.83 (1H, br d, J = 13.9 Hz), 2.02–2.11 (1H, m), 2.41 (3H, s), 2.56 (2H, q, J = 15.1, 7.6 Hz), 2.63–2.81 (5H, m), 2.94 (1H, dd, J = 10.8, 2.5 Hz), 4.40 (1H, dd, J = 11.5, 3.7 Hz), 5.23 (1H, d, J = 2.4 Hz), 7.08 (2H, d J = 8.0 Hz), 7.26 (2H, d, J = 8.3 Hz), 7.41 (2H, d, J = 8.3 Hz), 7.85 (2H, d, J = 8.1 Hz); ^{13}C NMR ($CDCl_3$) δ 14.9, 15.1, 28.5, 40.0, 45.8, 50.2, 51.4, 54.6, 72.3, 124.4, 127.6, 128.2, 128.5, 133.5, 142.3, 144.4, 150.9, 203.7. Anal. ($C_{23}H_{29}NO_2$) C, H, N.

2-Chlorophenyl 4-(2-chlorophenyl)-4-hydroxy-1-methyl-3-piperidyl ketone (16). White solid; yield 71%; mp 83–85 °C. ^{1}H NMR ($CDCl_3$) δ 1.58 (1H, br d, J = 13.7 Hz), 2.42 (3H, s), 2.66–2.82 (3H, m), 2.87–2.98 (1H, m), 3.04 (1H, dd, J = 11.0, 3.4 Hz), 4.60 (1H, d, J = 2.7 Hz), 5.22 (1H, dd, J = 11.5, 3.9 Hz), 6.94 (1H, d, J = 7.1 Hz), 7.07–7.12 (3H, m), 7.25–7.36 (3H, m), 7.92 (1H, d, J = 8.1 Hz); ^{13}C NMR ($CDCl_3$) 33.9, 46.1, 50.9, 51.4, 53.2, 73.1, 126.5, 127.0, 128.6, 128.8, 128.9, 130.3, 131.3, 131.5, 132.1, 138.2, 142.1, 207.2. Anal. ($C_{19}H_{19}Cl_2NO_2$) C, H, N.

3-Chlorophenyl 4-(3-chlorophenyl)-4-hydroxy-1-methyl-3-piperidyl ketone (17). Light-yellow solid; yield 68%; mp 115–117 °C. ^{1}H NMR ($CDCl_3$) δ 1.80 (1H, br d, J = 11.5 Hz), 1.98–2.09 (1H, m), 2.41 (3H, s), 2.63–2.72 (2H, m), 2.79 (1H, broad d, J = 7.0 Hz), 2.92 (1H, dd, J = 11.2, 2.9 Hz), 4.30 (1H, dd, J = 11.5, 3.7 Hz), 5.01 (1H, d, J = 2.4 Hz), 7.11–7.20 (2H, m), 7.30 (1H, d, J = 7.0 Hz), 7.39 (1H, t, J = 8.1 Hz), 7.53 (2H, d, J = 4.8 Hz), 7.70 (1H, d, J = 7.8 Hz), 7.84 (1H, s); ^{13}C NMR ($CDCl_3$) δ 39.7, 45.8, 50.8, 51.1, 54.3, 72.4, 122.4, 125.2, 126.3, 127.0, 128.3, 129.5, 130.1, 133.9, 134.4, 135.2, 137.1, 149.1, 202.6. Anal. ($C_{19}H_{19}Cl_2NO_2$) C, H, N.

3,4-Difluorophenyl 4-(3,4-difluorophenyl)-4-hydroxy-1-methyl-3-piperidyl ketone (18). White solid; yield 59%; mp 110–112 °C. ^{1}H NMR ($CDCl_3$) δ 1.80 (1H, br d, J = 13.9 Hz), 1.95–2.06 (1H, m), 2.41 (3H, s), 2.66 (2H, t, J = 11.2 Hz), 2.80 (1H, br dd, J = 8.8, 1.8 Hz), 2.92 (1H, dd, J = 11.2, 3.1 Hz), 4.23 (1H, dd, J = 11.2, 3.4 Hz), 5.03 (1H, d, J = 2.5 Hz), 6.99–7.15 (2H, m), 7.21–7.37 (2H, m), 7.68–7.74 (2H, m); ^{13}C NMR ($CDCl_3$) δ 39.7, 45.8, 50.5, 51.1, 54.4, 72.1, 114.1, 114.3, 116.9, 117.2, 117.5, 117.7, 118.0, 120.1, 120.2, 120.3, 125.3, 125.4, 125.5, 125.6, 132.6, 144.2, 147.5, 148.5, 150.6, 152.1, 152.3, 155.9, 201.2. Anal. ($C_{19}H_{17}F_4NO_2$) C, H, N.

3,4-Dimethylphenyl 4-(3,4-dimethylphenyl)-4-hydroxy-1-methyl-3-piperidyl ketone (19). Light-yellow solid; yield 76%; mp 90–92 °C. ^{1}H NMR ($CDCl_3$) δ 2.18 (1H, br d, J = 13.9 Hz), 1.99–2.10 (1H, m), 2.16 (3H, s), 2.20 (3H, s), 2.30 (3H, s), 2.31 (3H, s), 2.41 (3H, s), 2.63–2.80 (3H, m), 2.92 (1H, dd, J = 11.0, 2.8 Hz), 4.38 (1H, dd, J = 11.4, 3.6 Hz), 5.25 (1H, d, J = 2.7 Hz), 6.99 (1H, d, J = 7.8 Hz), 7.19 (2H, t, J = 7.1 Hz), 7.33 (1H, br s), 7.68 (2H, d, J = 7.4 Hz); ^{13}C NMR ($CDCl_3$) δ 19.2, 19.7, 19.9, 20.0, 40.3, 45.9, 50.1, 51.5, 54.7, 72.3, 121.6, 126.1, 126.2, 129.4, 129.5, 129.9, 133.7, 134.8, 136.2, 137.1, 143.7, 144.7, 204.0. Anal. ($C_{23}H_{29}NO\cdot HCl$) C, H, N.

4-Chloro-3-methylphenyl 4-(4-chloro-3-methylphenyl)-4-hydroxy-1-methyl-3-piperidyl ketone (20). White solid; yield 82%; mp 114–116 °C. ^{1}H NMR ($CDCl_3$) δ 1.80 (1H, d, J = 13.9 Hz), 1.99–2.08 (1H, m), 2.30 (3H, s), 2.40 (3H, s), 2.42 (3H, s), 2.64–2.81 (3H, m), 2.92 (1H, dd, J = 11.9 Hz, 3.4 Hz), 4.32 (1H, dd, J = 11.5, 3.7 Hz), 5.10 (1H, d, J = 2.4 Hz), 7.18 (2H, s), 7.40 (2H, t, J = 5.1 Hz), 7.66 (1H, dd, J = 8.3 Hz, 2.0 Hz), 7.75 (1H, s); ^{13}C NMR ($CDCl_3$) δ 20.1, 20.2, 39.8, 45.8, 50.3, 51.2, 54.4, 72.2, 123.1, 126.9, 127.4, 128.8, 129.5, 130.6, 132.7, 134.0, 135.7, 136.9, 140.9, 145.5, 203.0. Anal. ($C_{21}H_{23}Cl_2NO_2$·HCl) C, H, N.

1-Ethyl-4-hydroxy-4-(4-methylphenyl)-3-piperidyl 4-methylphenyl ketone (21). White solid; yield 60%; mp 115–117 °C. ^{1}H NMR ($CDCl_3$) δ 1.15 (3H, t, J = 7.3 Hz), 1.84 (1H, br d, J = 13.9 Hz), 1.99–2.10 (1H, m), 2.57 (3H, s), 2.41 (3H, s), 2.53–2.71 (4H, m), 2.90 (1H, broad d, J = 11.3 Hz), 3.00 (1H, dd, J = 11.2, 2.6 Hz), 4.36 (1H, dd, J = 11.5, 3.5 Hz), 5.24 (1H, d, J = 2.5 Hz), 7.06 (2H, d, J = 8.1 Hz), 7.24 (2H, d, J = 8.1 Hz), 7.40 (2H, d, J = 8.1 Hz), 7.82 (2H, d, J = 8.0 Hz); ^{13}C NMR ($CDCl_3$) δ 12.0, 20.7, 21.5, 40.0, 48.6, 50.1, 52.0, 52.5, 72.9, 124.3, 128.4, 128.8, 129.4, 133.3, 136.0, 144.3, 144.8, 203.9. Anal. ($C_{22}H_{27}NO_2$) C, H, N.

4-Chlorophenyl 4-(4-chlorophenyl)-1-ethyl-4-hydroxy-3-piperidyl ketone (22). White solid; yield 91%; mp 151 °C. ^{1}H NMR ($CDCl_3$) δ 1.14 (3H, t, J = 7.0 Hz), 1.82 (1H, br d, J = 13.9 Hz), 1.95–2.06 (1H, m), 2.53–2.71 (4H, m), 2.90 (1H, dd, J = 9.5, 1.7 Hz), 2.98 (1H, dd, J = 11.0, 2.5 Hz), 4.28 (1H, dd, J = 11.2, 3.4 Hz), 5.10 (1H, d, J = 2.4 Hz), 7.22 (2H, d, J = 8.5 Hz), 7.42 (4H, dd, J = 8.5, 1.7 Hz), 7.82 (2H, d, J = 8.8 Hz); ^{13}C NMR ($CDCl_3$) δ 12.0, 39.7, 48.4, 50.5, 52.0, 52.3, 72.9, 125.9, 128.4, 129.1, 129.6, 132.6, 133.9, 140.7. 145.6, 202.9. Anal. ($C_{20}H_{21}Cl_2NO_2$) C, H, N.

3,4-Dichlorophenyl 4-(3,4-dichlorophenyl)-1-ethyl-4-hydroxy-3-piperidyl ketone (23). White solid; yield 71%; mp 140 °C. ^{1}H NMR ($CDCl_3$) δ 1.11 (3H, t, J = 7.3 Hz), 1.78 (1H, br d, J = 14.0 Hz), 1.93–2.01 (1H, m), 2.50–2.67 (4H, m), 2.87 (1H, br d, J = 11.2 Hz), 2.95 (1H, dd, J = 11.0, 2.7 Hz), 4.19 (1H, dd, J = 11.2, 3.4 Hz), 4.97 (1H, d, J = 2.2 Hz), 7.21–7.30 (2H, m), 7.50 (1H, d, J = 8.3 Hz), 7.61 (1H, d, J = 1.9 Hz), 7.69 (1H, dd, J = 8.3, 1.9 Hz), 7.92 (1H, d, J = 2.0 Hz); ^{13}C NMR ($CDCl_3$) δ 11.9, 39.5, 48.1, 50.5, 51.9, 52.1, 72.6, 123.6, 127.1, 130.1, 130.2, 130.8, 130.9, 132.5, 133.7, 134.9, 138.9, 147.3, 201.4. Anal. ($C_{20}H_{19}Cl_4NO_2$) C, H, N.

3,4-Dichlorophenyl 4-(3,4-dichlorophenyl)-4-hydroxy-1-(2-phenylethyl)-3-piperidyl ketone (24). Light-yellow thick syrup; yield 67%. ^{1}H NMR ($CDCl_3$) δ 1.83 (1H, br d, J = 13.9 Hz), 1.96–2.07 (1H, m), 2.73–3.04 (8H, m), 4.22 (1H, dd, J = 11.2, 3.7 Hz), 4.98 (1H, d, J = 2.5 Hz), 7.22–7.35 (7H, m), 7.56 (1H, d, J = 8.6 Hz), 7.65 (1H, d, J = 2.2 Hz), 7.72 (1H, dd, J = 8.3, 2.0 Hz), 7.96 (1H, d, J = 2.2 Hz); ^{13}C NMR ($CDCl_3$) δ 33.6, 39.6, 48.7, 50.6, 52.4, 59.9, 72.7, 123.7, 126.1, 127.1, 127.2, 128.4, 128.6, 130.2, 130.3, 131.0, 132.7, 133.8, 135.0, 139.1, 139.8, 147.3, 201.5. Anal. ($C_{26}H_{23}Cl_4NO_2$·HCl) C, H, N.

4-Bromophenyl 4-(4-bromophenyl)-4-hydroxy-1-(2-phenylethyl)-3-piperidyl ketone (25). Yellow thick syrup; yield 74%. ^{1}H NMR ($CDCl_3$) δ 1.82 (1H, br d, J = 13.9 Hz), 1.97–2.08 (1H, m), 2.74–3.04 (8H, m), 4.28 (1H, dd, J = 11.2, 3.4 Hz), 5.08 (1H, d, J = 2.4 Hz), 7.21–7.38 (9H, m), 7.60 (2H, d, J = 8.6 Hz), 7.74 (2H, d, J = 8.5 Hz); ^{13}C NMR ($CDCl_3$) δ 33.6, 39.7, 48.9, 50.4, 52.5, 60.0, 72.9, 120.8, 126.1, 126.4, 128.4, 128.6, 129.6, 129.7, 131.4, 132.2, 134.3, 139.9, 146.1, 203.0. Anal. ($C_{26}H_{25}Br_2NO_2$) C, H, N.

3,4-Dichlorophenyl 4-(3,4-dichlorophenyl)-4-hydroxy-1-(3-phenylpropyl)-3-piperidyl ketone (26). Colorless thick syrup; yield 62%. ^{1}H NMR ($CDCl_3$) δ 1.77–2.02 (4H, m), 2.52 (2H, t, J = 7.8 Hz), 2.61–2.71 (4H, m), 2.86–2.96 (2H, m), 4.18 (1H, dd, J = 11.5, 3.7 Hz), 4.96 (1H, d, J = 2.4 Hz), 7.20–7.35 (7H, m), 7.56 (1H, d, J = 8.3 Hz), 7.63 (1H, d, J = 1.9 Hz), 7.71 (1H, dd, J = 8.6, 2.0 Hz), 7.95 (1H, d, J = 1.7 Hz); ^{13}C NMR ($CDCl_3$) δ 28.6, 33.7, 39.6, 48.7, 50.6, 52.5, 57.6, 72.7, 123.7, 125.8, 127.1, 128.3, 130.2, 130.3, 131.0, 131.1, 132.6, 133.8, 135.0, 139.1, 141.8, 147.4, 201.6. Anal. ($C_{27}H_{25}Cl_4NO_2$) C, H, N.

4-Bromophenyl 4-(4-bromophenyl)-4-hydroxy-1-(3-phenylpropyl)-3-piperidyl ketone (27). Yellow thick syrup; yield 69%. ^{1}H NMR ($CDCl_3$) δ 1.77–2.03 (4H, m), 2.52 (2H, t, J = 8.3 Hz), 2.63–2.71 (4H, m), 2.87 (1H, br d, J = 11.0 Hz), 2.95 (1H, dd, J = 11.0, 2.9 Hz), 4.26 (1H, dd, J = 11.2, 3.2 Hz), 5.08 (1H, d, J = 2.4 Hz), 7.20–7.41 (9H, m), 7.60 (2H, d, J = 8.3 Hz), 7.74 (2H, d, J = 8.6 Hz); ^{13}C NMR ($CDCl_3$) δ 28.7, 33.7, 39.7, 48.9, 50.4, 52.6, 57.6, 72.9, 120.8, 125.8, 126.3, 128.3, 128.4, 129.6, 129.7, 131.3, 132.2, 134.3, 141.8, 146.2, 203.0. Anal. ($C_{27}H_{27}Br_2NO_2$) C, H, N.

HPLC separation of enantiomers

Racemic piperidinols were separated into their individual enantiomers by using a chirex brand HPLC column (Chirex 3018, purchased from Phenomenex, Inc., CA) which contains (*S*)-proline covalently bound to γ-aminopropyl silinized silica gel (5 μm particle size) and derivatized via an urea linkage with (*R*)-1-(α-naphthyl)-ethylamine as a chiral stationary phase.[44] The chiral HPLC was performed on a Shimadzu SCL-10A-VP system at a flow rate of 5.0 mL/min at room temperature using hexane/DCM/ethanol-TFA (20-1) as a mobile phase in 87.5:10:2.5 ratio and UV detection at 254 and 280 nm. The sample for injection was prepared by dissolving racemic piperidinol (5 mg/1 mL) in mobile phase and the separation was carried out by injecting 250 μL on a 250×10 mm chiral column. Retention times and rotations of each isomer were given in Table 8.

Pharmacology

[^{3}H]Mazindol binding. Binding assays were conducted as previously described.[30] Briefly conventional P_2 membrane pellets were prepared by differential centrifugation from rat striatum. The P_2 pellet was resuspended in Krebs–Ringer-HEPES (KRH) buffer consisting of (in mM): NaCl (125), KCl (4.8), $MgSO_4$ (1.2), $CaCl_2$ (1.3),

Table 8. Retention times and rotations of each isomer

Compound	Isomer	Retention time (t_R) min	Optical rotation (°)	Concentration (%) and solvent
3	(+)-isomer	13.5	+54.0	0.5, DCM
	(−)-isomer	17.2	−54.0	0.5, DCM
4	(+)-isomer	14.9	+93.3	0.4, DCM
	(−)-isomer	18.2	−93.3	0.4, DCM
19	(+)-isomer	12.1	+44.2	1.0, DCM
	(−)-isomer	14.8	−44.2	1.0, DCM
20	(+)-isomer	18.2	+62.3	0.7, DCM
	(−)-isomer	22.4	−62.3	0.7, DCM

KH_2PO_4 (1.2), glucose (5.6), nialamide (0.01), and HEPES (25) (pH 7.4)[37] and centrifuged again. Finally, the pellet was resuspended in 30 volumes of buffer, pelleted at 15,000*g* and frozen at −80 °C until used. The striatal homogenates were thawed by resuspension in the buffer described above at 75–125 μg protein/mL and incubated with [^{3}H]mazindol, with or without competing drugs, for 60 min in a 4 °C cold room. Nonspecific binding was determined with 30 μM cocaine. The bound and free [^{3}H]mazindol were separated by rapid vacuum filtration over Whatman GF/C filters, using a Brandel M24R cell harvester, followed by two washes with 5 mL of cold buffer. Radioactivity on the filters was then extracted by allowing to sit over night with 5 mL of scintillant. The vials were vortexed and counted. IC_{50} values were determined using the computer program LIGAND.

Synaptosomal uptake of [^{3}H]DA, [^{3}H]SER, and [^{3}H]NE. The effect of candidate compounds in antagonizing dopamine high-affinity uptake was determined using a method previously employed.[30] For [^{3}H]DA uptake, dissected rat striata were homogenized with a Teflon-glass pestle in ice-cold 0.32 M sucrose and centrifuged for 10 min at 1000*g*. The supernatant was centrifuged at 17,500*g* for 20 min. This P_2 synaptosomal pellet was resuspended in 30 volumes of ice-cold modified KRH buffer. An aliquot of the synaptosomal suspension was preincubated with the buffer and drug for 30 min at 37 °C, and uptake initiated by the addition of [^{3}H]dopamine (5 nM, final concn.). After 5 min, uptake was terminated by adding 5 mL of cold buffer containing glucosamine as a substitute for NaCl and then finally by rapid vacuum filtration over GF-C glass fiber filters, followed by washing with two 5 mL volumes of ice-cold, sodium-free buffer. Radioactivity retained on the filters was determined by liquid scintillation spectrometry. Specific uptake is defined as that which is sensitive to inhibition by 30 μM cocaine. It is identical to that calculated by subtracting the mean of identical tubes incubated at 0 °C. [^{3}H]SER and [^{3}H]NE uptake were measured in an entirely analogous fashion using synaptosomes prepared from rat midbrain and parietal/occipital cortex, respectively. Also, specific uptake of [^{3}H]SER and [^{3}H]NE were defined in the presence of 10 uM fluoxetine and 1 uM desipramine, respectively.

IC_{50} values were determined by a computer assisted, iterative fit to a four-parameter sigmoidal equation (ALLFIT). These values were then converted to K_i values according to the Cheng–Prusoff equation assuming classical competitive inhibition. Pre-incubation of the drug and synaptosomes at 37 °C for 30 min was used to approximate equilibrium conditions as necessary to satisfy the requirements of the Cheng–Prusoff equation.

Functional antagonism. The IC_{50} value of cocaine in the presence of approximate IC_{10}–C_{50} concentrations of candidate antagonist compounds was then compared to the IC_{50} value of cocaine alone. Significant differences in

Elemental analysis

Compound	Molecular formula	Calculated			Found		
		C	H	N	C	H	N
12	$C_{19}H_{19}C_{l2}NO_2$	62.65	5.26	3.85	62.51	5.16	3.63
13	$C_{19}H_{19}Br_2NO_2$	50.36	4.23	3.09	50.57	4.35	3.12
14	$C_{19}H_{19}I_2NO_2$	41.71	3.50	2.56	41.80	3.59	2.66
15	$C_{23}H_{29}NO_2$	78.59	8.32	3.99	78.44	8.29	3.88
16	$C_{19}H_{19}Cl_2NO_2$	62.65	5.26	3.85	62.63	5.34	3.72
17	$C_{19}H_{19}Cl_2NO_2$	62.65	5.26	3.85	62.77	5.28	3.88
18	$C_{19}H_{17}F_4NO_2$	62.12	4.66	3.81	61.99	4.72	3.79
19	$C_{23}H_{29}NO_2 \cdot HCl$	71.21	7.79	3.61	71.11	7.71	3.72
20	$C_{21}H_{23}Cl_2NO_2 \cdot HCl$	58.82	5.64	3.27	58.69	5.60	3.15
21	$C_{22}H_{27}NO_2$	78.30	8.06	4.15	78.21	8.00	4.14
22	$C_{20}H_{21}Cl_2NO_2$	63.50	5.60	3.70	63.35	5.44	3.60
23	$C_{20}H_{19}Cl_4NO_2$	53.75	4.28	3.13	53.66	4.31	3.07
24	$C_{26}H_{23}Cl_4NO_2 \cdot HCl$	55.79	4.32	2.50	55.61	4.31	2.39
25	$C_{26}H_{25}Br_2NO_2$	57.48	4.64	2.58	57.53	4.71	2.64
26	$C_{27}H_{25}Cl_4NO_2$	60.35	4.69	2.61	60.47	4.81	2.69
27	$C_{27}H_{27}Br_2NO_2$	58.19	4.88	2.51	58.07	4.74	2.42
29	C_9H_9ClO	64.11	5.38		64.02	5.30	

IC_{50} values were compared to theoretical IC_{50} values expected from models of 'same site' antagonism.[33,34] IC_{50} values greater than those expected for 'same site' antagonism was taken as evidence of functional antagonism. Compounds demonstrating antagonism were tested at lower concentrations to determine their minimum effective concentration. This test was performed under the preincubation conditions described above to allow slowly equilibrating compounds to reach equilibrium. Further, any artifactual differences in K_i due to differences in temperature, tissue preparation, and so on, were negated in this assay as binding of cocaine and the putative antagonists to both the cocaine binding site and the transporter occurred under identical conditions. This insures that a right shift in the cocaine inhibition curve beyond what is expected for two drugs acting at the same site is a true measure of functional antagonism.

Acknowledgements

This work is supported by a grant (DA-11545) from the National Institute on Drug Abuse, National Institutes of Health. We wish to thank Dr. Tivadar Farkas of Phenomenex, Inc. 2320 W. 205th Street, Torrance, CA 90501, USA for his help on the design of the chiral HPLC column used in this work.

References and Notes

1. Carroll, F. I.; Howell, L. L.; Kuhar, M. J. *J. Med. Chem.* **1999**, *42*, 2721.
2. Ritz, M. C.; Lamb, R. J.; Goldberg, S. R.; Kuhar, M. J. *Science* **1987**, *237*, 1219.
3. Carroll, F. I.; Lewin, A. H.; Boja, J. W.; Kuhar, M. J. *J. Med. Chem.* **1992**, *35*, 969.
4. Kuhar, M. J.; Ritz, M. C.; Boja, J. W. *Trends Neurosci.* **1991**, *14*, 299.
5. Lin, Z.; Wang, W.; Kopajtic, T.; Revay, R.; Uhl, G. *Mol. Pharmacol.* **1999**, *56*, 434.
6. Woolverton, W. L.; Johnson, K. M. *TIPS* **1992**, *13*, 193.
7. Woolverton, W. L.; Kleven, M. S. *NIDA Research Monograph* **1988**, *88*, 160.
8. Spealman, R. D.; Madras, B. K.; Bergman, J. *Pharmacol. Exp. Ther.* **1989**, *251*, 142.
9. Carroll, F. I.; Lewin, A. H.; Biswas, J. *Pharm. News* **1994**, *1*, 11.
10. Wise, R. A. *Brain Res.* **1978**, *152*, 215.
11. Carroll, F. I.; Kotian, P.; Dehghani, A.; Gray, J. L.; Kuzemko, M. A.; Parham, K. A.; Abraham, P.; Lewin, A. H.; Boja, J. W.; Kuhar, M. J. *J. Med. Chem.* **1995**, *38*, 379.
12. Carroll, F. I.; Gray, J. L.; Abraham, P.; Kuzemko, M. A.; Lewin, A. H.; Boja, J. W.; Kuhar, M. J. *J. Med. Chem.* **1993**, *36*, 2886.
13. Meltzer, P. C.; Liang, A. Y.; Madras, B. K. *J. Med. Chem.* **1994**, *37*, 2001.
14. Newman, A. H.; Kline, R. H.; Allen, A. C.; Izenwasser, S.; George, C.; Katz, J. L. *J. Med. Chem.* **1995**, *38*, 3933.
15. Kozikowski, A. P.; Roberti, M.; Xiang, L.; Bergmann, J. S.; Callahan, P. M.; Cunningham, K. A.; Johnson, K. M. *J. Med. Chem.* **1992**, *35*, 4764.
16. Kozikowski, A. P.; Saiah, M. K. E.; Bergmann, J. S.; Johnson, K. M. *J. Med. Chem.* **1994**, *37*, 3440.
17. Smith, M. P.; Johnson, K. M.; Zheng, M.; Flippen-Anderson, J. L.; Kozikowski, A. P. *J. Am. Chem. Soc.* **1998**, *120*, 9072.
18. Lieske, S. F.; Yang, B.; Eldefrawi, M. E.; MacKerell, A. D., Jr.; Wright, J. *J. Med. Chem.* **1998**, *41*, 864.
19. Chen, Z.; Izenwasser, S.; Katz, J. L.; Klein, C. L.; Zhu, N.; Trudell, M. L. *J. Med. Chem.* **1996**, *39*, 4744.
20. Glowa, J. R.; Fantegrossi, W. E.; Lewis, D. B.; Matecka, D.; Rice, K. C.; Rothman, R. B. *J. Med. Chem.* **1996**, *39*, 4689.
21. Matecka, D.; Rothman, R. B.; Radesca, L.; de Costa, B.; Dersch, C. M.; Partilla, J. S.; Pert, A.; Glowa, J. R.; Wojnicki, F. H. M.; Rice, K. C. *J. Med. Chem.* **1996**, *39*, 4704.
22. Matecka, D.; Lewis, D.; Rothman, R. B.; Dersch, C. M.; Wojnicki, F. H. E.; Glowa, J. R.; DeVries, A. C.; Pert, A.; Rice, K. C. *J. Med. Chem.* **1997**, *40*, 705.
23. Deutsch, H. M.; Shi, Q.; Gruszecka-Kowalik, E.; Schweri, M. M. *J. Med. Chem.* **1996**, *39*, 1201.
24. Houlihan, W. J.; Boja, J. W.; Parrino, V. A.; Kopajtic, T. A.; Kuhar, M. J. *J. Med. Chem.* **1996**, *39*, 4935.
25. Singh, S.; Basmadjian, G. P.; Avor, K. S.; Pouw, B.; Seale, T. W. *J. Med. Chem.* **1997**, *40*, 2474.
26. Avor, K. S.; Singh, S.; Seale, T. W.; Pouw, B.; Basmadjian, G. P. *J. Med. Chem.* **1998**, *41*, 2380.
27. (a) Kozikowski, A. P.; Araldi, G. L.; Boja, J.; Meil, W. M.; Johnson, K. M.; Flippen-Anderson, J. L.; George, C.; Saiah, E. *J. Med. Chem.* **1998**, *41*, 1962. (b) Tamiz, A. P.; Zhang, J.; Flippen-Anderson, J. L.; Zhang, M.; Johnson, K. M.; Deschaux, O.; Tella, S.; Kozikowski, A. P. *J. Med. Chem.* **2000**, *43*, 1215.
28. Sakamuri, S.; Enyedy, I. J.; Kozikowski, A. P.; Zaman, W. A.; Johnson, K. M.; Wang, S. *Bioorg. Med. Chem. Lett.* **2001**, *11*, 495.
29. Smith, M. P.; Hoepping, A.; Johnson, K. M.; Trzcinska, M.; Kozikowski, A. P. *Drug Discovery Today* **1999**, *7*, 322.
30. Wang, S.; Sakamuri, S.; Enyedy, I. J.; Kozikowski, A. P.; Deschaux, O.; Bandyopadhyay, B. C.; Tella, S. R.; Zaman, W. A.; Johnson, K. M. *J. Med. Chem.* **2000**, *43*, 351.
31. Prakash, K. R. C.; Tamiz, A. P.; Araldi, G. L.; Zhang, M.; Johnson, K. M.; Kozikowski, A. P. *Bioorg. Med. Chem. Lett.* **1999**, *9*, 3325.
32. Meltzer, P. C.; Blundell, P.; Madras, B. K. *Med. Chem. Res.* **1998**, *8*, 12.
33. Huang, L.-Y. M.; Ehrenstein, G. *J. Gen. Physiol.* **1981**, *77*, 37.
34. Reith, M. E. A.; Selmeci, F. *Naunyn-Schmiedeberg's Arch. Pharmacol.* **1992**, *345*, 309.
35. Ono, A. Fujimoto, E.; Ueno, M. *Synthesis* **1986**, 570.
36. Dimmock, J. R.; Vashishtha, S. C.; Wilson Quail, J.; Pugazhenthi, U.; Zimpel, Z.; Sudom, A. M.; Allen, T. M.; Kao, G. Y.; Balzarini, J.; De Clercq, E. *J. Med. Chem.* **1998**, *41*, 4012.
37. Slusher, B. S.; Tiffany, C. W.; Olkowski, J. L.; Jackson, P. F. *Drug Alcohol Depend.* **1997**, *48*, 43.
38. QUANTA, a molecular modeling system, is supplied by Molecular Simulations Inc., 9685 Scranton Road, San Diego, CA 92121-3752, USA.
39. Brooks, B. R.; Bruccoleri, R. E.; Olafson, B. D.; States, D. J.; Swaminathan, S.; Jaun, B.; Karplus, M. *J. Comput. Chem.* **1983**, *4*, 187.
40. Nicklaus, M. C.; Wang, S.; Driscoll, J.; Milne, G. W. A. *Bioorg. Med. Chem.* **1995**, *3*, 411.
41. Cerius^2, a molecular modeling system, is supplied by Molecular Simulations Inc., 9685 Scranton Road, San Diego, CA 92121-3752, USA.
42. Rogers, D.; Hopfinger, A. J. *J. Chem. Inf. Comput. Sci.* **1994**, *34*, 854.
43. Ghose, A. K.; Pritchett, A.; Crippen, G. M. *J. Comput. Chem.* **1988**, *9*, 180.
44. Cleveland, T. *J. Liq. Chromatogr.* **1995**, *18*, 649.